

# SQUID MULTIPLEXERS FOR TRANSITION-EDGE SENSORS

Mikko Kiviranta<sup>a</sup>, Jan van der Kuur<sup>b</sup>, Heikki Seppä<sup>a</sup>, Piet de Korte<sup>b</sup>

<sup>a</sup>VTT Microsensing, Otakaari 7B, 02150 Espoo, Finland

<sup>b</sup>SRON, Sorbonnelaan 2, 3584 CA Utrecht, the Netherlands

## ABSTRACT

SQUID-based multiplexing readout circuitry for thermal radiation detectors using superconducting phase transition thermometers is reviewed and some design choices are considered. The emphasis is on the frequency domain multiplexing scheme for X-ray calorimeter arrays.

## INTRODUCTION

The combination of good energy resolution, fast response, and good absorption cross-section makes the Transition Edge Sensor (TES) a good candidate for single photon counters at X-ray energies.

Some sort of a multiplexing scheme would be highly advantageous in attempts to build X-ray cameras with a large number of pixels. Without multiplexing, the readout electronics would be complex and fragile, and the large number of wires would easily lead into too high heat leakage. The recent achievement<sup>1</sup> of 6.9 eV energy resolution for 5.89 keV photons with an ac-biased TES is one milestone suggesting feasibility of frequency-domain multiplexed readouts for such X-ray camera missions as XEUS by the European Space Agency.

## MULTIPLEXING

### Basis functions

In multiplexing schemes the signals are fingerprinted by multiplying them with an orthogonal set of functions of time, and added to a common wire. Demultiplexing is performed by multiplying with the fingerprinting functions again so that the desired signal can be picked from the common wire. This is reminiscent of how basis functions pick out pre-coefficients from superpositions in Quantum Mechanics, e.g.  $\langle f_2 | \times (c_1 | f_1 \rangle + c_2 | f_2 \rangle + c_3 | f_3 \rangle + \dots) = c_2$ . In QM the analogy of signals are the ‘dc’ coefficients  $c_1, c_2 \dots$  but when realistic time-dependent signals  $c_1(t), c_2(t) \dots$  are multiplexed, one must choose basis functions such that multiplication products won’t overlap in the used basis. For example, if one uses sinusoids as the basis, their separation in frequency must be at least twice the bandwidth of each signal. Among possible basis functions, sines and cosines (for Frequency Domain Multiplexing, FDM) and differently delayed pulse trains (for Time Domain Multiplexing, TDM) are most popular, but other choices, e.g. wavelets or Hadamard functions are possible.

### Modulators

The two devices capable of performing the multiplication, which are naturally present in a readout circuit, are the TES and the SQUID. TES-based modulators utilize Ohm’s law to multiply signal-dependent conductivity with fingerprint-carrying bias voltage into a current signal. TES kinetic inductance can be used instead of resistance<sup>2</sup>. SQUID-based modulators utilize bias-dependence of the gain  $\partial V / \partial \Phi$  to multiply the signal-dependent input flux with fingerprint-carrying SQUID bias.

### Need for filters

TDM and FDM behave differently when wideband noise is added to the signal. In FDM, the noise added before modulator and after the modulator stand on the same footing, as multiplying a signal by a sinusoid simply shifts all the signals by the sinusoid frequency in the frequency space. Thus it is sufficient to have a

band-pass filter just before the summing point, in order to avoid folding of the noise to adjacent channels and subsequent degradation of the signal-to-noise ratio (SNR), see Fig. 1.

In TDM already the input signal has to be frequency-limited, because the effective integration time for noise is the short on-time time  $t_A$  of the channel, but the signal is sampled more slowly: on the intervals  $N t_A$  in a  $N$ -channel multiplexer.

At the output of a TES, the signal and the phonon noise are band-limited by thermal cutoff, but Johnson noise is not band-limited. The signal node between the modulator and addition of the Johnson noise is not accessible, so that the low-pass filter needed in TDM cannot be implemented if TES is used as the modulator. It is conceivable, however, to accept the resulting  $\sqrt{N}$  penalty in SNR but make the Johnson noise lower by driving at each moment the off-state TESes to high-resistance state above transition by magnetic switching. When SQUID is used as the modulator, the above-mentioned signal node is accessible and the pre-modulator low-pass filter can be installed there. Generally the TES resistance  $R_{TES}$  and the SQUID input inductance are used to form a natural filter.

There's still a  $\sqrt{N}$  noise penalty present in the TDM, associated with the noise added after the modulator, (e.g. SQUID noise) which could be cured by using pulsed TES bias. The TES bias power should be concentrated on the active timeslots (just like power is concentrated only on active frequency bands in FDM), which would increase signal compared to Johnson and SQUID noises. The *average* bias power would still be limited by thermal conductivity and bath-to-transition temperature difference.

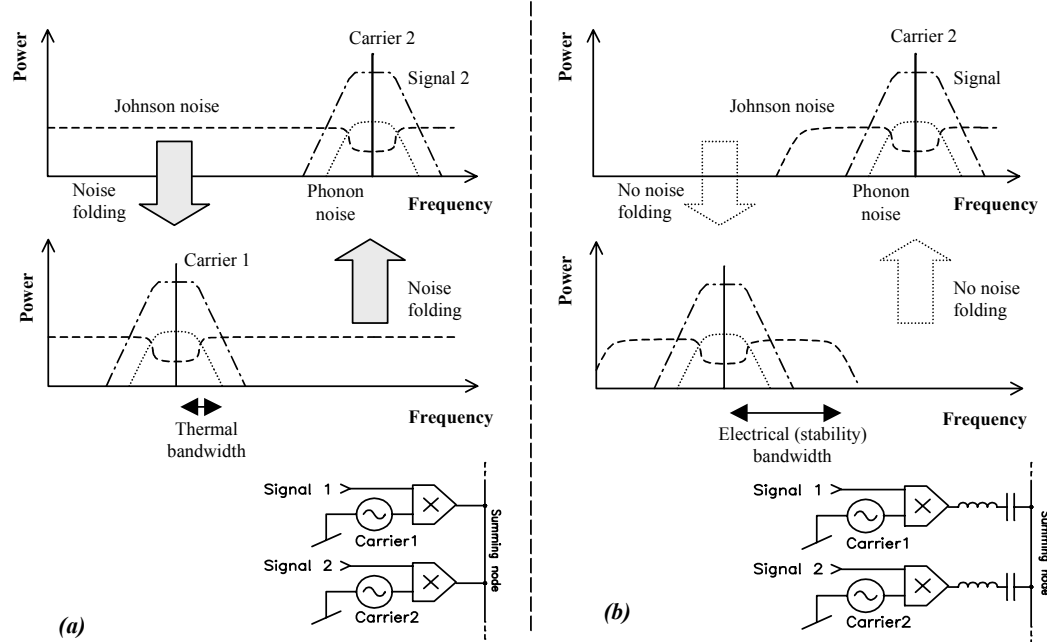


**Figure 1:** Signal spectra in frequency domain multiplexing without (a) and with (b) filter, when TES is used as the modulator.

## READOUT CONFIGURATIONS

### Single-pixel readout

The readout designer is given a set of active devices capable of giving genuine power gain, which he/she should combine in such a manner that (i) enough signal power is delivered at the output of the circuit so that further processing of the data is easy; (ii) dynamic ranges of the devices, i.e. ratios of the maximum signals to noise floors, are overlapped as shown in figure 2; and (iii) sufficient bandwidth is reached at each stage. The set of active devices usually consists of the TES, the SQUID, and the room-temperature (RT) amplifier. Each of these has the characteristic natural power gain, bandwidth, dynamic range, and input-referred noise power. The designer can use (short or long) negative feedback to trade power gain for dynamic range and bandwidth (DR&BW). Similarly, the designer can use positive feedback to trade DR&BW for power gain - for instance, to increase the noise power at the output of the first device above the input-referred noise power of the second device. Generally, short positive feedback need to be accompanied with a long negative feedback in order to restore the original DR&BW.

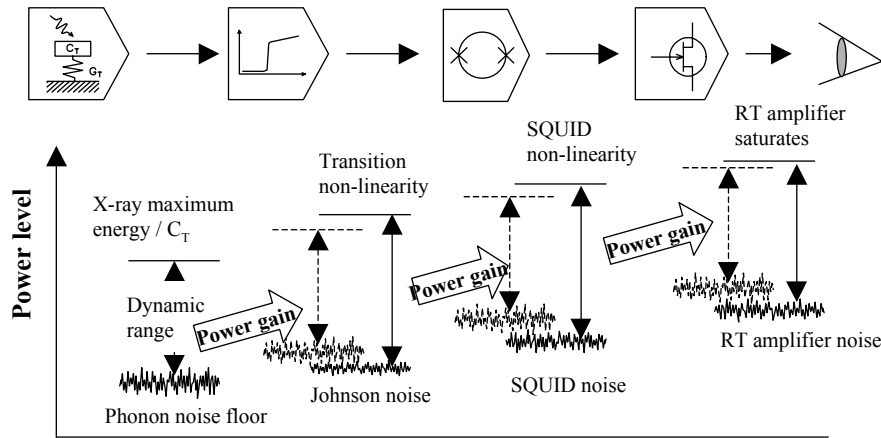


**Figure 2:** The designers task: matching dynamic ranges and noise floors.

As a side effect of using negative (positive) feedback, the generalized input and output impedances of the devices are modified. Depending on whether series or shunt feed is used, the input impedance either increases or decreases. Similarly the shunt or series output sampling circuit defines whether output impedance increases or decreases. These impedance transformations can be useful in performing impedance matching between the stages, primarily to obtain noise matching<sup>1</sup>, and secondarily to obtain power matching (if noise performance remains sufficient). Impedance transformations not associated with power gain can be performed with ordinary transformers, where necessary.

The most widely used TES readout configuration combines short negative feedback from TES output to TES input, so called electrothermal feedback (ETF), and negative feedback from output of RT amplifier to input of the SQUID, so called flux-locked loop. This is by no means the only configuration. As an example, one might use TES with constant power bias (no local feedback) and add negative feedback from RT amplifier to the TES input through a heater or a SINIS cooler.

### Multiplexed readout

In multiplexing readout separate signal paths are needed up to the location of modulators and summing point in the signal chain. After the summing point only single signal path is present, but bandwidth requirement is multiplied by the number of channels.

If feedback path crosses the summing point, demultiplexing of the feedback signals is necessary. Often demultiplexing takes place automatically. For example, in TDM scheme described in<sup>3</sup> only biased (active) SQUIDs respond to the feedback flux, and effectively perform demultiplexing of the feedback.

In the remaining sections we concentrate on the frequency-domain scheme with voltage-biased TESes showing strong ETF.

## FILTER IMPLEMENTATION

The noise blocking filters for the FDM should be compact enough to be integrated on the same substrate with the TES array. If wiring from the TES chip to a separate filter circuit was necessary, the key advantage over TDM would be lost. Ideally, the filters should reside at the crossings of the XY wiring matrix to the TES pixels, but due to lack of room they must in practice be fanned out to the surrounding substrate area.

In the case of TDM, the SQUIDs which typically act as noise-blocking filters for the pulse-train basis, are difficult to fabricate on the same chip with TESes, so that  $N$  wires for  $N$ -pixel array are needed between the TES chip and SQUID chip. An attractive but technologically challenging alternative would be to use through-wafer holes and bump bonding for inter-chip connection. Bumps on the same side of the washer

<sup>1</sup> Note that feedback does not affect the noise matching impedance (ratio of voltage and current noises or their generalizations) at device input, so that it is only useful to modify the output impedance of preceding stage by feedback in order to meet the noise matching impedance of the subsequent stage.

as absorbers force one to flip the detector chip face down, which is feasible in sub-mm wave detectors, but which in X-ray detectors would lead to loss of low-energy photons passing the support membrane. Straightforward LC resonators are most attractive filters for FDM, even though more exotic devices such as acoustic MEMS filters and active filters using SQUID as the amplifier are conceivable. The value of series inductance  $L$  is determined by stability condition: the  $R_{TES}/L$  ratio sets the filter settling time and if this is longer than the thermal time constant, a thermal instability occurs. This is a version of the dc stability condition<sup>4</sup> centered at carrier frequency rather than at dc. Presence of magnetic switching with ac bias makes analytic stability calculations hard, but one can resort to numerical simulations (Fig. 3)

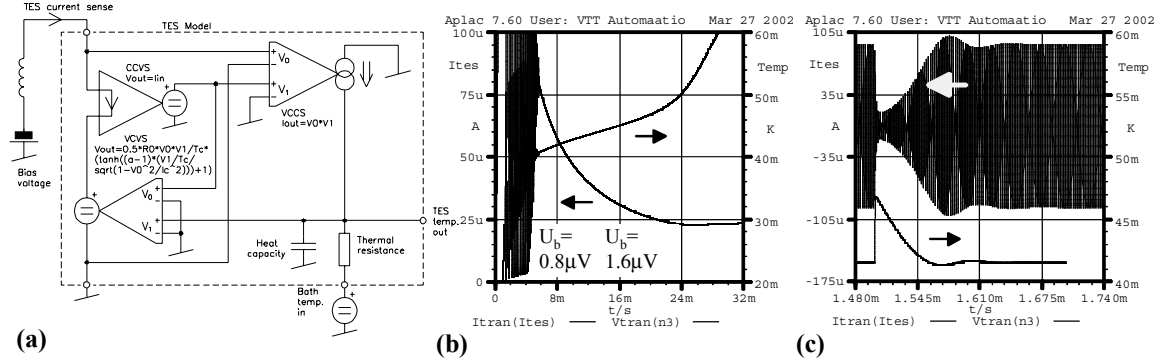


**Figure 3:** (a) TES model with Ginzburg-Landau magnetic switching for time domain and harmonic balance simulations in the (Spice-like) circuit simulator Aplac. (b) Current and temperature of a TES as a function of bias voltage. Bias circuit inductance is  $L=40$  nH, thermal conductance  $G_T = 1.1 \times 10^{-9}$  W/K, thermal capacitance  $C_T = 0.3 \times 10^{-12}$  J/K and transition width 6.8 mK. Thermal instability is seen when bias voltage  $U_b < 0.6 \mu\text{V}$  where  $R_{TES}/L < G_T/C_T$ . (c) Same TES ac-biased at 500 kHz with  $U_b = 0.7 \mu\text{V}$  rms through a 40 nH / 2.5  $\mu\text{F}$  LC-filter shows moderate ringing when a 10 keV photon arrives

Count rate requirement of 100cps per pixel for the XEUS mission combined with peak energy to energy resolution ratio of 10keV/2eV defines the thermal time constant of  $\sim 50 \mu\text{s}$  and sets a limit  $L < 40$  nH for our TESes with  $R_{TES} = 10 \text{ m}\Omega$  at bias point. Footprint for such an integrated inductor is  $d \approx 4.2 \times \sqrt[3]{w^2 L / \mu_0}$  or  $210 \times 210 \mu\text{m}$  when lithographic linewidth is assumed to be  $w=2 \mu\text{m}$ .

Inductors cannot be packed close to each other, because inductor-to-inductor mutual coupling has the same effect as common inductance after the summing point. Any common inductance, stray or intentional, limits the total bandwidth available to the frequency channels. Transforming inductors into radial gradiometers by surrounding them with superconducting guard rings allows packing the inductors into  $\sim 1 \times 1$  mm grid and still having sufficiently low coupling. The total TES/filter chip dimension for a  $32 \times 32$  pixel array would then be reasonable  $\sim 35 \times 35$  mm.

The capacitance  $C$  defines the carrier frequency. A 0402-cased ceramic multilayer capacitor, bump-soldered directly on the TES/filter chip, has a footprint of  $0.5 \times 1$  mm and a typical value in the order of a few nF at 4.2K. Similar capacitances per area can be achieved with integrated capacitors using  $\text{Nb}_2\text{O}_5$  ( $\sim 10$  nF/ $\text{mm}^2$ ), twin-layer  $\text{Ta}_2\text{O}_5$  ( $\sim 25$  nF/ $\text{mm}^2$ ) or Nb/ $\text{AlOx}$ /Nb trilayers ( $\sim 40$  nF/ $\text{mm}^2$ ) as dielectric, with the benefits of assuredly superconducting plates (reduced effective series resistance) and improved reliability.  $0.5 \times 1$  mm  $\text{Nb}_2\text{O}_5$  capacitors would set the carrier frequency at  $\sim 11$  MHz. If internal thermal fluctuation noise turns out not to limit the energy resolution, TES resistance can conceivably be increased from  $10 \text{ m}\Omega$  to, say,  $100 \text{ m}\Omega$  which would allow  $\sim 4$  MHz operation with same capacitor size. The center frequency can be further lowered by enlarging the chip area.

Tolerance of the capacitors becomes critical when a large number of resonators is fed from a single generator tuned at a single frequency. A mis-tuned resonator not only attenuates the signal but can also lead to TES instability. Thin dielectrics required for large capacitance make it hard to produce low-tolerance capacitors.

The primary purpose of LC filters is to prevent noise folding. The ultimate frequency response of each multiplexed channel, which also determines channel-to-channel crosstalk, is set by post-detection filters.

## DYNAMIC RANGE

The dynamic range of the TES output current is determined by the required ratio of maximum photon energy to energy resolution, and the thermal time constant  $I_{\max}/I_n = 2.36 \times E_{\max}/(\Delta E_{FWHM} \sqrt{\tau})$ , or  $\sim 1.7 \times 10^6$  for XEUS requirements when dc bias is used. In FDM the peak-to-peak current is  $2\sqrt{2}$  times the RMS current, so that dynamic range needs to be increased accordingly.

### SQUID in open loop

Theoretically, the natural dynamic range of a SQUID is the ratio of half flux quantum to the flux noise  $\Phi_n = k_c^{-1} \sqrt{2L_{SQ}\epsilon} = k_c^{-1} \sqrt{2L_{SQ}(\eta + 12k_B T \sqrt{L_{SQ}C_j})}$ . With SQUID loop inductance  $L_{sq} \approx 5$  pH, achievable by standard photolithography, the critical current density of  $J_c = 10^7$  A/m<sup>2</sup> and capacitance density of  $C_D = 0.05$  F/m<sup>2</sup> in the tunnel barrier sheet would lead<sup>#</sup> to junction capacitance  $C_j \sim 1$  pF and to quantum-limited operation at  $T < 300$  mK, if no excess noise was present. A reasonable value of the magnetic coupling constant  $k_c$  would then lead to dynamic range in the order of  $10^7$ , barely sufficient for typical requirements for X-ray calorimeters, especially when the need for linearizing the response is taken into account. Because the SQUID is naturally rather well matched to the low impedance of the TES, the input coil of the SQUID shall have a low number of turns which makes it easier to avoid excess noise associated with input coil resonances. *Absolute* value of input-referred current noise of the SQUID can be adjusted by changing the number of turns, but the number can be increased only up to the point where back-action noise starts to dominate. The *ratio* of maximum current to current noise only depends on SQUID loop parameters in the thermally-limited domain:  $I_{\max}/I_n \sim L_{SQ}^{-3/4} C_j^{-1/4}$  in both SQUID-limiting and amplifier-limiting cases. In

some cases the dynamic range is constrained by the dissipated power  $P_{diss} \sim (I_{\max}/I_n)^2$ .

When the energy resolution  $\epsilon$  is either quantum limited or limited by barrier sheet properties  $\epsilon = 12k_B T \sqrt{\Phi_0 C_D / 2J_c}$ , dynamic range can still be improved by reducing loop impedance. Three ways to do this are (i) to use e-beam lithography for loop definition, (ii) to couple several loops in parallel (Fig. 4a), or (iii) to use an array SQUID. Computation of circuit parameters shows that a series array made of  $k$  SQUIDs, each having loop inductance  $L_{sq}$ , junction capacitance  $C_j$  and an  $n$ -turn input coil, is equivalent to a single SQUID with loop inductance  $L_{sq}/k$ , junction capacitance  $kC_j$ , equipped with an  $nk$ -turn input coil and an  $1:k$  transformer at its output (Fig. 4b). The effective reduction of  $L_{sq}$  then implies  $\sqrt{k}$ -fold improvement in dynamic range.

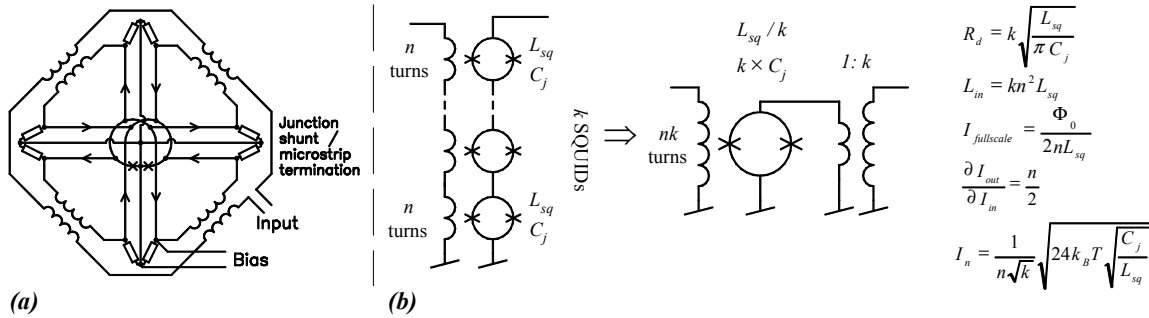


**Figure 4:** (a) A multiloop SQUID. (b) Equivalence between  $k$ -SQUID series array and a single SQUID.

<sup>#</sup> Note the constraint  $\beta_L = 2I_c L_{SQ} / \Phi_0 \leq 1$ .

## SQUID with negative feedback

The feasibility of negative feedback depends crucially on implementable center frequency of the noise-blocking filters. If one local oscillator (LO) cycle is much shorter than round-trip cable delay to room-temperature electronics and back, straightforward negative feedback can be used. A non-standard controller such as integrator-and-half<sup>5</sup> can help to attain the high dynamic range at high frequencies<sup>1</sup>. Shunt-in feedback topology (current injection or flux injection) results in as an additional benefit the decrease of input inductance, including stray inductance in the signal path after the feedback summing point.

If filter design forces one to use high LO frequency, one can resort to (i) use of a cryogenic semiconductor amplifier located close to the SQUIDs, or (ii) arranging negative feedback through room temperature only in the narrow band close to the LO frequency (Fig. 5). A disadvantage of high-frequency operation is that the noise power at the SQUID input increases as a function of frequency.

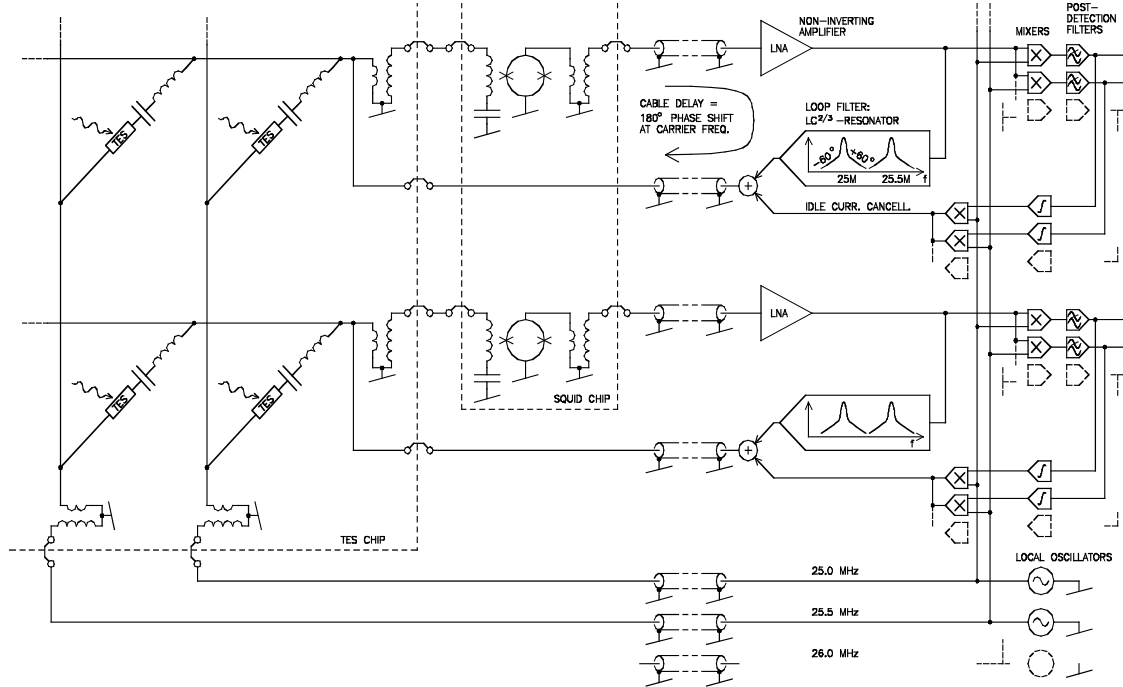


**Figure 5:** Schematic diagram of FDM readout circuitry using low-C filters and narrowband feedback.

## CONCLUSION

Practical TDM multiplexers are operational now, but would need to be improved in order to meet the high-speed, large dynamic range specifications of XEUS. Feasibility of practical FDM multiplexers depends on implementation of a filtering scheme which would be scalable to large numbers of pixels and would allow sufficiently low carrier frequencies. Both FDM and TDM would benefit from SQUID controllers having a large dynamic range at high frequencies. Ultimate theoretical performance of FDM and TDM does not differ from each other, and the choice between the two should be based on implementability considerations.

## REFERENCES

1. Jan van der Kuur et al, submitted to Appl. Phys. Lett.
2. Heikki Seppä, IEEE Tran. Appl. Supercond. vol. 11, no. 1, pp. 759-761, March 2001.
3. Kent Irwin, Physica C, vol. 368, pp. 203-210, 2002.
4. Kent Irwin et al, J. Appl. Phys. vol. 83, no. 8, pp. 3978-3985, 15 April 1998.
5. Heikki Seppä and Hannu Sipola, Rev. Sci. Instr. vol. 61, no. 9, pp. 2449-2451, Sept. 1990.

<sup>1</sup> The often-cited figure of merit, the slew rate, is fully meaningful only when open-loop frequency response of the controller is that of the simple integrator.